PHYSICAL REVIEW B **90**, 184405 (2014)

Terahertz emission spectroscopy of laser-induced spin dynamics in $TmFeO_3$ and $ErFeO_3$ orthoferrites

R. V. Mikhaylovskiy,[1,*] E. Hendry,[2] V. V. Kruglyak,[2] R. V. Pisarev,[3] Th. Rasing,[1] and A. V. Kimel[1]

[1]*Radboud University Nijmegen, Institute for Molecules and Materials, Heyendaalseweg 135, 6525 AJ Nijmegen, the Netherlands*

[2]*School of Physics, University of Exeter, Stocker Road, Exeter EX4 4QL, United Kingdom*

[3]*Ioffe Physical-Technical Institute, Russian Academy of Sciences, 194021 St. Petersburg, Russia*

(Received 22 July 2014; revised manuscript received 23 September 2014; published 5 November 2014)

Using the examples of laser-induced spin-reorientation phase transitions in $TmFeO_3$ and $ErFeO_3$ orthoferrites, we demonstrate that terahertz emission spectroscopy can obtain novel information about ultrafast laser-induced spin dynamics, which is not accessible by more common all-optical methods. The power of the method is evidenced by the fact that, in addition to the expected quasi-ferromagnetic and quasi-antiferromagnetic modes of the iron sublattices, terahertz emission spectroscopy enables detection of a resonance optically excited at an unexpected frequency of ~0.3–0.35 THz. By recording how the amplitude and phase of the excited oscillations depend on temperature and applied magnetic field, we show that the unexpected mode has all the features of a spin resonance of the Fe^{3+} ions. We suggest that it can be assigned to transitions between the multiplet sublevels of the ${}^6A_1$ ground state of the Fe^{+3} ions occupying rare-earth positions.

DOI: 10.1103/PhysRevB.90.184405 PACS number(s): 75.78.Jp, 78.20.Ls, 75.30.Kz

I. INTRODUCTION

Ultrafast effects of light on spins in magnetic materials, optical control of magnetism, and all-optical magnetic recording are intensively discussed topics of contemporary magnetism [1]. The abundance of magnetic phases and optomagnetic phenomena in magnetic insulators offers a wide perspective for the development of high-speed magnetic recording technologies and the custom design of spintronic devices operating at terahertz (THz) frequencies [2,3]. Moreover, the spin resonances in insulators have inherently smaller damping compared to the magnetic metals, which makes them attractive for the technologies relying on propagating spin waves [4].

The rare-earth orthoferrites $RFeO_3$ (R stands for a rare-earth ion), although discovered more than 60 years ago [5], have recently become a model system for modern physics of magnetism [6] and multiferroicity [7–9]. In particular, they offer a rich playground for the investigation of optical control of magnetism in magnetic insulators. In the visible spectral range, magneto-optical spectroscopies and pump-probe measurements have enabled a substantial advance in the understanding of the effects that ultrashort optical pulses can have on spins. In these experiments, a femtosecond laser pump pulse excites the magnetic medium, while another laser pulse, delayed with respect to the pump, probes the photo-induced magnetic changes via the magneto-optical Faraday and/or Cotton-Mouton effects. Examples of successful studies of these types are the ultrafast light-induced spin reorientation in antiferromagnets [10–13], ultrafast inverse Faraday effect [14–16], and inertia-driven switching [17]. However, a substantial limitation of these techniques lies in the fact that visible light cannot interact with spins directly, enabling access only to those spin resonances that efficiently couple to the orbital degree of freedom via the spin-orbit interaction. As a result, the information about spin dynamics obtained using all-optical pump-probe techniques is quite limited, which often becomes a source of controversy in the area of femtosecond magnetism [18–21].

At the same time, the magnetic component of THz radiation can couple directly to the spin resonances. It has been demonstrated that broadband pulses of THz radiation can serve as a probe of spin resonances in $YFeO_3$ [22–24], $ErFeO_3$ [25], $NdFeO_3$ [26], and $Tb_3Ga_5O_{12}$ [27]. A promising approach to control magnetic order with the help of intense-enough THz pulses has been suggested for NiO [28]. Conversely, laser-induced spin dynamics in magnetic materials is also accompanied by emission of the THz radiation [29–36]. Here we show that THz emission spectroscopy provides novel information about ultrafast laser-induced spin dynamics in $TmFeO_3$ and $ErFeO_3$ orthoferrites which is not accessible by more common all-optical methods [10–12]. The power of the method is evidenced by the fact that, in addition to the expected quasi-ferromagnetic and quasi-antiferromagnetic modes of the iron sublattices, the THz emission spectroscopy enables detection of an optically excited resonance at an unexpected frequency of ~0.3–0.35 THz.

II. EXPERIMENT AND RESULTS

The main advantage of the THz emission spectroscopy is its ability to detect all magnetic and electric dipole oscillations at THz frequencies excited by ultrashort laser pulses. The second advantage of this technique is the possibility of an enhancement of the emission in a certain frequency domain. The THz emission conditions depend strongly on the dielectric environment of the sample, its refractive index, and thickness. Let us consider an infinite slab of a material with magnetization oscillating with frequency $\omega/2\pi$, i.e. $m(t) = m_0 e^{i\omega t}$. By solving Maxwell's equations for the slab of the material with a thickness d and the refractive index n, we find the amplitude of the emitted electric field into free space (in cgs units) as

$$E_0 = 4\pi m_0 \left[\frac{2n + (1-n)e^{-ikd} - (n+1)e^{ikd}}{(n-1)^2 e^{-ikd} - (n+1)^2 e^{ikd}} \right], \quad (1)$$

*R.Mikhaylovskiy@science.ru.nl

where $k = \frac{\omega}{c}n$, and c is the speed of light in vacuum. As one can see from Eq. (1), the emitted electric field depends on the frequency and is determined by the Fabry-Perot factor enclosed in square brackets. Consequently, the sensitivity of the THz emission spectroscopy to spin dynamics in a chosen spectral range can be enhanced by tuning the frequency of the Fabry-Perot resonance [37].

Here we employ the THz emission spectroscopy for studying the mechanisms of ultrafast optical control of magnetism in $TmFeO_3$ and $ErFeO_3$ orthoferrites. The THz spectrometer employed in our experiments was powered by an amplified Ti:sapphire laser emitting a sequence of optical pulses (800 nm wavelength, ~100 fs duration) with 1 kHz repetition frequency and is described elsewhere [27]. Following excitation by femtosecond optical pulses with a peak fluence of $\sim 10\,\mathrm{mJ/cm^2}$ and focused to spot of ~1 mm radius, $TmFeO_3$ and $ErFeO_3$ demonstrate ultrafast spin-reorientation dynamics, which we resolve by monitoring THz emission signals. We show that the THz emission spectroscopy serves as an alternative and complementary tool with respect to the more conventional all-optical pump-probe spectroscopy applied to study these materials previously [10–12]. Moreover, the power of this technique is evidenced here by the observation of an as yet unobserved optical excitation of dipole active modes in the vicinity of the spin-reorientation phase transition.

Orthoferrites have an orthorhombically distorted perovskite structure containing four iron ions and four rare-earth ions per crystallographic unit cell. Conventionally, the four iron spins are reduced to two antiferromagnetically coupled magnetic sublattices. However, the iron sublattices are not exactly antiparallel. Instead, they are slightly canted by an angle of 0.5° due to the Dzyaloshinskii-Moriya antisymmetric exchange interaction. The Néel temperature for the iron spins is about ~650 K. In contrast, the Tm and Er spins in the orthoferrites are ordered only below ~4 K. Since the magnetic anisotropy in rare-earth orthoferrites is characterized by a strong temperature dependence, various phase transitions can take place [38]. For example, $TmFeO_3$ and $ErFeO_3$ exhibit a spin reorientation in the ~80–95 K temperature interval. In the so-called Γ_2 magnetic phase below $T_1 = 80$ K, the magnetic anisotropy leads to alignment of the antiferromagnetic spins along the z axis, with a weak ferromagnetic moment $\mathbf{M}$ oriented along the x axis. Above $T_2 = 91$ K in $TmFeO_3$ and 95 K in $ErFeO_3$, the anisotropy favors the spin orientation along the x axis with a weak magnetic moment along the z axis (Γ_4 magnetic phase). In the temperature range between T_1 and T_2, the spin configuration continuously rotates in the (xz) plane while keeping the weak ferromagnetic moment in the same plane (the intermediate magnetic phase Γ_{24}).

The two-sublattice model of the magnetic structure of the orthoferrites predicts two eigenmodes: a low-frequency quasi-ferromagnetic (q-FM) mode at ~100–300 GHz and a high-frequency quasi-antiferromagnetic (q-AFM) mode at ~800 GHz [39]. The quasi-ferromagnetic mode conserves the angle between the magnetic sublattices (i.e., the weak ferromagnetic magnetization precesses with a constant length), while the quasi-antiferromagnetic mode does not (i.e., the weak ferromagnetic magnetization does not precess but its length oscillates).

The THz wave forms generated in a 60 μm-thick $TmFeO_3$ crystalline plate cut perpendicular to the z axis at different temperatures are shown in Fig. 1(a). The signal was observed only below 70 K, when the sample was in the Γ_2 phase. The THz emission spectrum consists of three narrow spectral components with frequencies of ~0.1 THz, ~0.35 THz, and ~0.8 THz, as can be seen from the representative spectrum acquired at 60 K and shown in Fig. 1(b). The values of the highest and lowest frequencies in this spectrum are in excellent agreement with those expected for quasi-antiferromagnetic and quasi-ferromagnetic modes of the iron sublattices, respectively [39]. However, optical excitation of the third mode observed at ~0.35 THz has not been previously reported in $TmFeO_3$. The emitted THz electric field was linearly polarized along the y axis of the crystal, which implies that the magnetic field is parallel to the x axis and is therefore also parallel to the magnetization $\mathbf{M}$ in the Γ_2 phase. The spectral components have different temperature dependences, as shown in Fig. 1(c).

The spectral component at 0.8 THz, which we assign to the quasi-antiferromagnetic mode of the iron sublattices, is observed at all temperatures below 70 K and its central frequency is weakly dependent of temperature, as one expects for the quasi-antiferromagnetic mode [39]. The polarization of the magnetic field of this component parallel to the magnetization suggests that it was directly emitted by the oscillating magnetic moment in the Γ_2 phase. Above the spin-reorientation temperature, the magnetization lies out-of-plane, along the z axis, and thus does not emit along this direction.

The spectral component at 0.1 THz, which we assign to the quasi-ferromagnetic mode of the iron sublattices, is excited in the relatively narrow temperature interval between 50 and 70 K. It is natural to assume that this mode is excited just below the spin-reorientation temperature range, as was observed in optical experiments [10–12]. The shift of ~20 K from the spin-reorientation region (80–90 K) is due to the steady-state temperature buildup via cumulative laser heating. Indeed, by taking the values of the thermal conductivity of the orthoferrite from the literature [40], we estimate that laser pumping with an average power of 100 mW leads to the sample heating over ~10 K [41]. We confirm this conclusion by comparing the temperature behavior of the excited modes at different pump powers, as shown in Fig. 2. As one can see, the decrease of the pump power by a factor of 2 shifts the temperature interval in which the quasi-ferromagnetic mode is excited by ~15 K towards the spin-reorientation region. It also leads to a similar shift of the onset temperature of the quasi-antiferromagnetic mode.

The unexpected spectral feature at 0.35 THz is observed in the same temperature range as the quasi-ferromagnetic mode. The magnetic field associated with this component is polarized along the x axis, in agreement with the hypothesis that this is a magnetic mode. Hence this 0.35 THz mode has all the features similar to those of the quasi-ferromagnetic mode, suggesting that the mode must be associated with the iron spins. To confirm the suggested origin of the modes we have repeated the measurements on the x-cut and the y-cut $ErFeO_3$ crystalline plates.

Terahertz emission spectroscopy measurements on $ErFeO_3$ samples reveal spectral peaks similar to those described above. The representative spectrum of the THz emission at 55 K

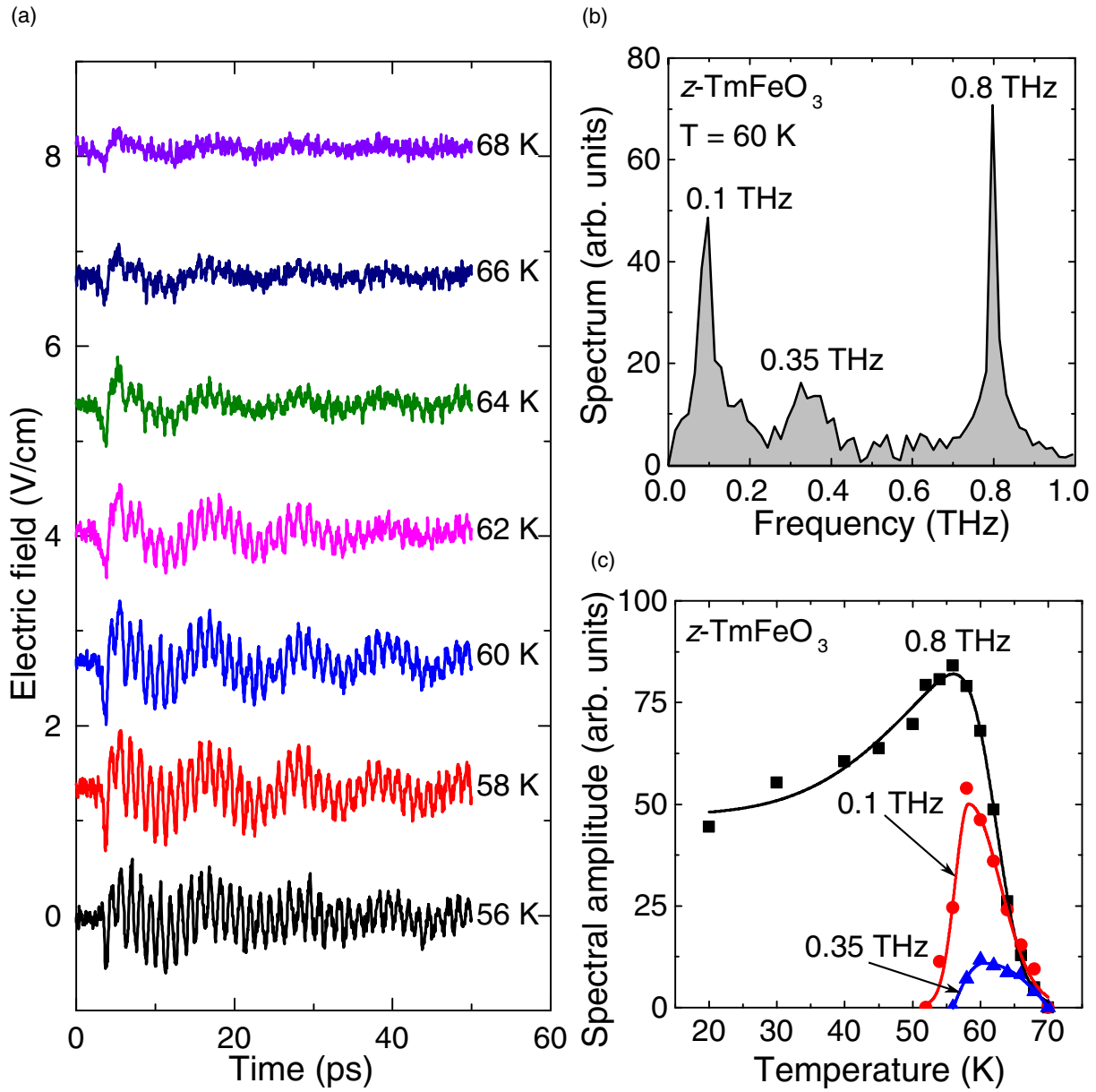

FIG. 1. (Color online) (a) The typical wave forms optically generated in the z-cut $TmFeO_3$. (b) The Fourier spectrum of the THz wave form generated in $TmFeO_3$ at 60 K. One can clearly observe three spectral peaks which we attribute to the quasi-ferromagnetic mode at 0.1 THz, the quasi-antiferromagnetic mode at 0.8 THz, and an unexpected resonance at 0.35 THz. (c) The amplitudes of the three spectral components of the THz emission spectra: the quasi-ferromagnetic mode (red circles), the unexpected mode (blue triangles), and quasi-antiferromagnetic mode (black squares) are shown as functions of temperature. Lines are guides for the eye.

is shown in Fig. 3(a). It contains three spectral features at ~0.15 THz, ~0.3 THz, and ~0.75 THz. As before, the THz radiation is polarized as expected for a magnetic dipole emission, and does not depend on the pump polarization. Again, we attribute the lowest-frequency mode to the emission arising from a photo-induced quasi-ferromagnetic precession, while the highest-frequency mode at 0.75 THz is attributed to the emission due to the photo-excited quasi-antiferromagnetic mode. The mode observed here in $ErFeO_3$ at 0.3 THz is attributed to the same origin as the unexpected mode observed in $TmFeO_3$ at ~0.35 THz. The temperature dependences of the spectral peak amplitudes are shown in Fig. 3(b) for $ErFeO_3$ cut perpendicular to the x axis, while very similar dependences were observed also for the y-cut $ErFeO_3$ sample. In the x-cut $ErFeO_3$, the ~0.75-THz peak is observed above the spin-reorientation temperature. In the y-cut sample, this mode can be observed at any temperature but its polarization rotates by 90° from the x to the z axis with the spin reorientation, as the temperature increases from 50 to 65 K. The reversal of the applied magnetic field and magnetization of the sample leads to a sign change of the measured signal that confirms the magnetic nature of all observed modes [Fig. 4(a)]. Measurements performed at different temperatures and for different polarizations of the optical excitation showed that the

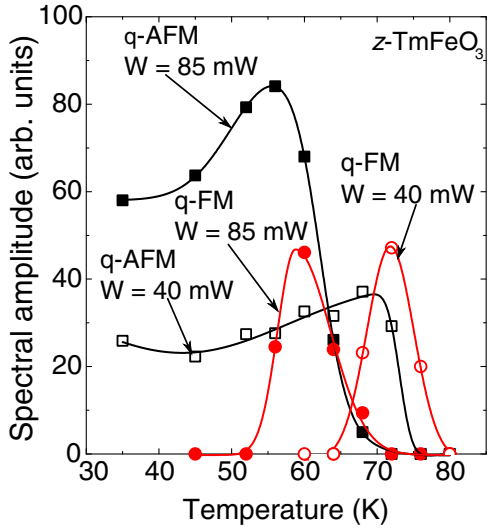

FIG. 2. (Color online) The spectral amplitudes of the quasi-antiferromagnetic (q-AFM) and quasi-ferromagnetic (q-FM) modes measured for two different values of the pump power W (85 and 40 mW) in the z-cut $TmFeO_3$ sample are shown as functions of temperature. The lines are guides for the eye.

emitted THz radiation is independent of the pump polarization at all temperatures. The example of the signal for two opposite pump helicities is shown in Fig. 4(b).

III. DISCUSSION

Our observations reveal that the quasi-antiferromagnetic mode is effectively excited both below [Fig. 1(c)] and above [Fig. 3(b)] the spin-reorientation temperature interval. Therefore the excitation mechanism does not rely on the crossing of the spin-reorientation temperature. Instead, it is likely to result from an optomagnetic effect such as optical perturbation of the exchange interaction by the pump pulse via an inverse magnetorefractive effect [42]. It is important to emphasize that the excitation of this mode has not been observed optically in $TmFeO_3$ and $ErFeO_3$, in contrast to the quasi-ferromagnetic mode [10–12]. The latter is excited only just below the temperature interval of the spin-reorientation phase transition. As explained in Refs. [10–12], such behavior is typical for modes excited due to laser-induced heating over the spin-reorientation temperature, and thus the heating induced modification of the magnetic anisotropy. If the initial temperature is just below the spin-reorientation region, the photo-induced modification of the anisotropy changes the equilibrium orientation of the spins. Thus the spins begin to precess around a new equilibrium orientation.

The relatively broad and weak peak at 0.3–0.35 THz has a temperature dependence that is similar to that of the quasi-ferromagnetic mode. This suggests that excitation of the mode also relies on thermal heating near the spin-reorientation phase transition. Although the THz emission spectroscopy measurements clearly reveal that the mode is excited in both $TmFeO_3$ and $ErFeO_3$, it has never been observed before in either optical pump-probe measurements [10–12] or in time-domain THz absorption spectroscopy [25]. The appearance of

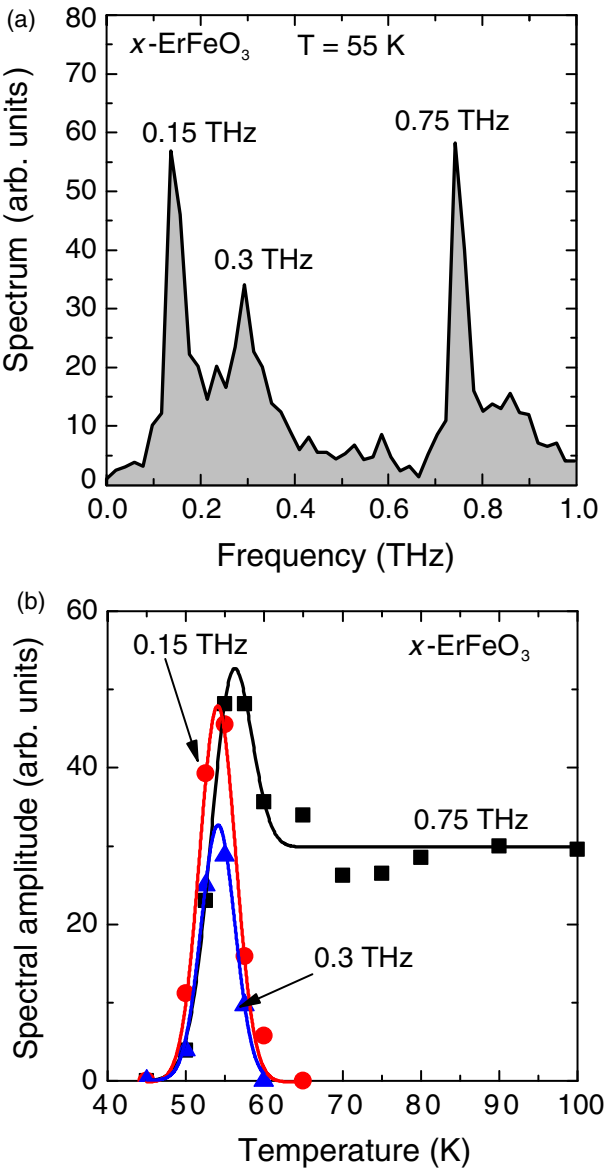

FIG. 3. (Color online) (a) The Fourier spectrum of the THz wave form generated in the x-cut $ErFeO_3$ at 55 K. Three spectral lines are distinguishable: the quasi-ferromagnetic mode at 0.15 THz, the unexpected peak at 0.3 THz, and the quasi-antiferromagnetic mode at 0.75 THz. (b) The amplitudes of the three spectral components of the THz emission spectra—the quasi-ferromagnetic mode (red circles), the unexpected mode (blue triangles), and the quasi-antiferromagnetic mode (black squares) are shown as functions of temperature. Lines are guides for the eye.

this formerly unobserved spectral peak would suggest that the laser-induced spin dynamics of the orthoferrites may be more complicated than previously thought [43]. Moreover, it also raises a question about the origin of this mode.

Since the magnetic structure of the orthoferrites contains four iron sublattices, two "hidden" modes are expected beside the quasi-ferromagnetic and quasi-antiferromagnetic modes [44]. However, the frequencies of these two modes are defined by the exchange interactions only and are expected to be much higher than 1 THz. Moreover, the theory from Ref. [44]

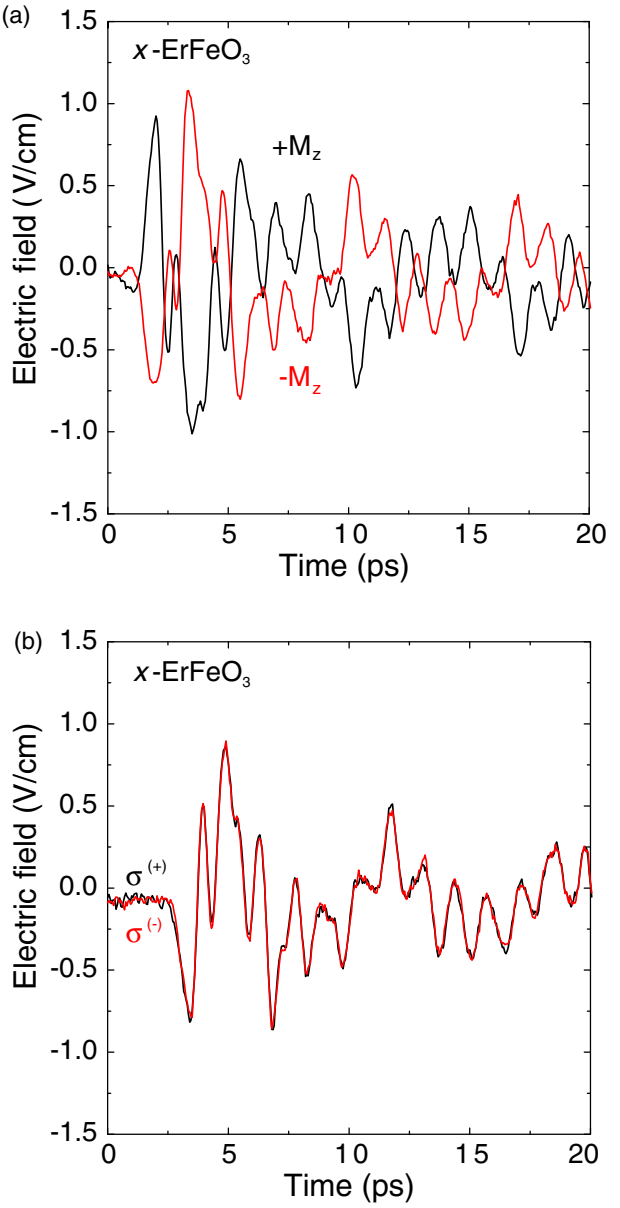

FIG. 4. (Color online) (a) The THz wave forms generated in the x-cut $ErFeO_3$ for opposite orientation of the magnetization along the z axis. (b) The THz wave forms generated in the x-cut $ErFeO_3$ for opposite helicities of the circularly polarized pump.

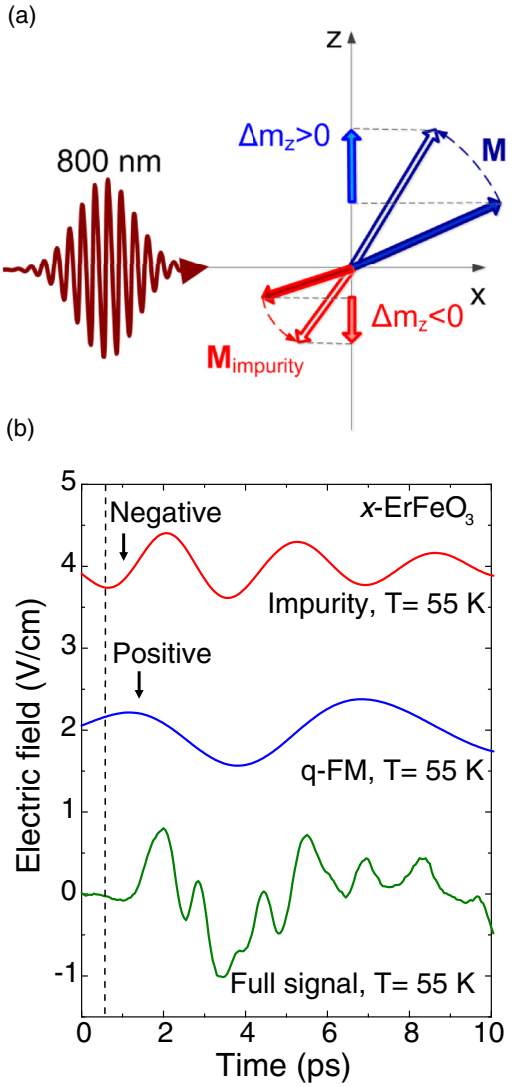

FIG. 5. (Color online) (a) The motion of the iron sublattice magnetization and the magnetization of the impurities (exaggerated for clarity) due to the laser-induced spin reorientation in the x-cut sample. The initial changes of the normal magnetization and the magnetization of the impurities are opposite. (b) The electric field generated in the x-cut $ErFeO_3$ sample at 55 K is shown along with its components arising from the quasi-ferromagnetic mode (q-FM) and the impurity modes. These contributions have opposite initial phases at a certain time delay just after the laser excitation as shown by a dashed vertical line.

predicts that these modes are magnetic dipole active along the y axis, while we did not observe emission with a magnetic field polarized along the y axis. Furthermore, the ground multiplets of both Er^{+3} and Tm^{+3} ions reported in the literature do not contain any transition close to ~0.3 THz [45–47].

Submillimeter spectroscopy of an isostructural compound $YFeO_3$ has revealed a few modes in the frequency interval between 250 and 300 GHz [48,49]. These modes were attributed to transitions within the ground state ${}^6A_1$ multiplet of Fe^{+3} ions occupying rare-earth positions as "impurities." Interestingly, despite a very small concentration of the impurities (~0.01% per formula unit), their relevant absorption peaks are reported to be only 1 order of magnitude smaller than the peak corresponding to the quasi-ferromagnetic mode [49]. Our THz emission spectroscopy setup does not have sufficient spectral resolution to distinguish several impurity modes close to each other. As such, they can be seen as one broad spectral feature around 0.3 THz.

According to Ref. [49], the iron impurities are magnetically polarized antiparallel to the magnetization of the "pure" iron sublattices. The light-induced perturbation of the magnetic anisotropy and the subsequent change of the equilibrium orientation of the magnetization $\mathbf{M}$ must lead to the associated change of the equilibrium orientation of the impurities as shown in Fig. 5(a). Therefore the magnetization of the impurities $\mathbf{M}_{imp}$ starts to rotate towards the new equilibrium

position, resulting in the excitation of the paramagnetic modes of the impurities. The change of the impurity magnetization $\mathbf{M}_{\text{imp}}$ during the initial motion is opposite with respect to the initial motion of the magnetization $\mathbf{M}$. Since the THz emission spectroscopy is sensitive to the phase of the signals, we compare the initial signs of the first half cycles of the quasi-ferromagnetic mode and the impurity modes [Fig. 5(b)]. To separate their contributions to the full signal, we apply the low-pass filter (cutoff frequency 200 GHz) and band-pass filter (cutoffs at 200 and 600 GHz) to the data. The resulting wave forms are shown in Fig. 5(b). One can see that these modes commence with different phases of the first half cycles. Indeed, the first half cycle of the quasi-ferromagnetic mode is negative, while the first half cycle of the impurity mode is positive. This observation is compatible with the proposed model of the orientation of the impurity spins [Fig. 5(a)]. We note that the unexpected modes could also arise from the Fe^{2+} ions which may substitute the Fe^{3+} ions in the crystal, even in the normal positions, and act as additional impurities.

Let us emphasize the differences between the optical detection of the laser-induced spin dynamics described in Refs. [10–12] and the THz emission spectroscopy reported here. As a matter of fact, in the experiments in which the laser-induced spin dynamics in the orthoferrites is detected with the help of the magneto-optical techniques, such as the Faraday effect or the Cotton-Mouton effect, the low-frequency mode of spin resonance is much stronger than the modes with higher frequencies. Consequently, the quasi-antiferromagnetic mode and the impurity modes can be easily overlooked. In order to explain why these modes are much easier to detect using the THz emission spectroscopy, we use Eq. (1). It neglects the retardation of radiation due to the finite speed of the optical pump pulse and can be applied in a context of light-induced magnetization dynamics only if the samples are thin enough to be traversed by the laser pulse faster than the characteristic time of the magnetization dynamics, such as the periods of the magnetic resonance modes. The thickness of our samples is $d = 60$ μm and 70 μm for the $TmFeO_3$ and $ErFeO_3$, respectively, and that guaranties the validity of Eq. (1), since the light propagation time over such a distance is $\sim$200 fs, which is much shorter than the periods of the observed oscillations. Using the measured amplitude of the electric field and values of the refractive index of the orthoferrites $n \approx 5$ taken from Ref. [39], we estimate the amplitude of the emitting magnetization m_0 to be $\sim$0.01, $\sim$0.0001, and $\sim$0.001 emu/cm^3 for the quasi-ferromagnetic mode, impurity modes, and the quasi-antiferromagnetic mode, correspondingly. Thus, while the amplitudes of the emitted electric fields are comparable for these modes (Figs. 1 and 2), the inferred magnetization amplitudes are orders of magnitude different. We thus may conclude that the enhancement of the emission arising from the quasi-antiferromagnetic mode and especially from the impurity modes is due to the Fabry-Perot resonances in the vicinity of the frequencies of these modes, as was also experimentally verified in our THz transmission measurements (see Appendix). The amplitude of the quasi-ferromagnetic oscillations measured in our THz spectrometer is of the same order of magnitude as in Refs. [11] and [12]. However, the quasi-antiferromagnetic mode and the impurity modes must have been orders of magnitude smaller in the optical signals and therefore might have been overlooked.

IV. SUMMARY

To summarize, we have unambiguously demonstrated that THz emission spectroscopy opens new opportunities in the studies of laser-induced magnetization dynamics. In particular, we demonstrated that this approach may serve as an independent, alternative and/or supplementary tool for disclosing processes that escape and are not revealed in all-optical pump-probe experiments. Although we confirm the ultrafast spin-reorientation transition observed optically, by monitoring THz emission we have also observed the unexpected impurity modes in both $TmFeO_3$ and $ErFeO_3$. We have also observed the optically triggered quasi-antiferromagnetic mode which has not been resolved previously in all-optical pump-probe experiments on these materials. The differences are likely to be due to the Fabry-Perot enhancement of these modes in the present experiments and highlight the complementarity of the THz emission spectroscopy compared to the all-optical spectroscopy. These differences must be taken into account in the design and interpretation of future experiments for resolving the multiple controversies in the broad research field of femtosecond magnetism.

ACKNOWLEDGMENTS

We acknowledge the help of A. van Roij, D. Malik, and T. J. Huisman in setting up the experiment on $ErFeO_3$. The research leading to these results was partially funded by the European Commission's 7th Framework Program (FP7/2007–2013) under Grant Agreement No. 228673 (MAGNONICS) and from EPSRC of the UK under Project No. EP/E055087/1. The work was partially supported by The Netherlands Organization for Scientific Research (NWO), the Foundation for Fundamental Research on Matter (FOM), the European Union's Seventh Framework Program (FP7/2007–2013) under Grants No. NMP3-LA-2010-246102 (IFOX) and No. 280555 (GoFast), and the European Research Council under the European Union's Seventh Framework Program (FP7/2007–2013) and ERC Grant Agreements No. 257280 (Femtomagnetism) and No. 339813 (EXCHANGE). R.V.P. acknowledges partial support from the Russian Government under Grant No. 14.B25.0031.25 and the RFBR under Grant No. 12-02-00130a.

APPENDIX

In addition to the THz emission spectroscopy measurements, we applied the conventional THz time-domain spectroscopy to our samples. In this technique a single-cycle broadband pulse of electromagnetic radiation passes through the sample. As a result, the temporal profile of the transmitted pulse is modied as compared to that of the incident pulse. The latter can be regarded as a reference. By analyzing absorption peaks in the normalized Fourier spectra of the pulses transmitted through the sample, one can obtain information about the spectrum of THz excitations in the sample. The details of the time-domain THz spectroscopy setup can be found elsewhere [22–27].

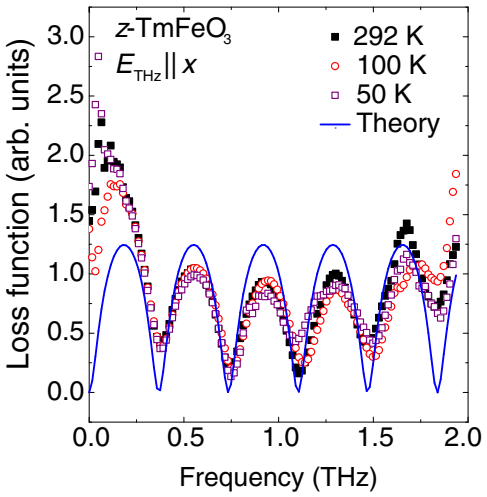

FIG. 6. (Color online) Loss functions of the z-cut $TmFeO_3$ at different temperatures measured for the incident THz electric field parallel to the x axis (symbols) are shown together with the theoretical function.

We analyze the THz transmission through the sample in terms of the normalized loss function $\sigma(\omega)$, defined as

$$\sigma(\omega) = -\ln\left(\left|\frac{S(\omega)}{S_{\mathrm{ref}}(\omega)}\right|\right), \tag{A1}$$

where $S(\omega)$ is the spectrum of the THz signal transmitted through the sample and $S_{\mathrm{ref}}(\omega)$ is the spectrum of the reference signal. The loss function accounts for both reflective and absorptive effects.

The indicative absorption spectra expressed in terms of the loss function $\sigma(\omega/2\pi)$ are shown in Fig. 6 for the z-cut $TmFeO_3$ sample. The loss functions for all samples and incident THz polarizations are very similar and share the same main feature. The response is dominated by the deep periodic minima of the background of the loss function.

In order to elucidate the origin of this oscillatory behavior, we found the ratio between the spectrum transmitted through the slab of the material with thickness d and refractive index n and the incident spectrum as

$$R(\omega) = \frac{4n}{(1+n)^2 e^{-ikd} - (1-n)^2 e^{ikd}}, \tag{A2}$$

where $k = \frac{\omega}{c}n$, as in Eq. (1). The loss function $\sigma_{F-P}(\omega) = -\ln|R(\omega)|$ describes only the losses due to the effects of the reflections at the sample faces. The theoretical function $\sigma_{F-P}(\omega/2\pi)$ calculated for $nd = 408$ μm is shown in Fig. 6 together with experimental loss functions. One can see that the oscillatory behavior of the loss function can be assigned to the factor given by Eq. (A2). This behavior arises due to the multiple reflections of the THz pulse inside the sample which result in a series of Fabry-Perot resonances. It should be noted, however, that the refractive index of $TmFeO_3$ $n \approx 5$ reported in the literature [39] gives a smaller value of the optical thickness $nd \approx 300$ μm. We attribute this discrepancy to the fact that Eq. (A2) is derived assuming propagation of the plane waves at normal incidence, while the THz pulse propagating through the sample in the real experiments is focused by a parabolic mirror. Therefore the THz beam propagates over a longer effective thickness compared to the effective thickness nd. Nevertheless, the loss function clearly shows the dominant role of the Fabry-Perot behavior in the samples under consideration. However, the function $R(\omega)$ differs from the Fabry-Perot factor in Eq. (1), since in the former case the source of THz waves is situated outside the sample at only one side of it, while in the latter situation the emitter (magnetization) is located inside the sample and the waves emitted at opposite interfaces of the sample can annihilate each other. Therefore the period of the Fabry-Perot factor in Eq. (1) is doubled compared to the period of the $R(\omega)$ function.

[1] J. Stöhr and H. C. Siegmann, *Magnetism: From Fundamentals to Nanoscale Dynamics* (Springer, Berlin, 2006).
[2] A. Kirilyuk, A. V. Kimel, and Th. Rasing, Rev. Mod. Phys. **82**, 2731 (2010).
[3] L. J. Heyderman and R. L. Stamps, J. Phys.: Condens. Matter. **25**, 363201 (2013).
[4] V. V. Kruglyak, S. O. Demokritov, and D. Grundler, J. Phys. D: Appl. Phys. **43**, 264001 (2010).
[5] R. M. White, J. Appl. Phys. **40**, 1061 (1969).
[6] S. Artyukhin, M. Mostovoy, N. P. Jensen, D. Le, K. Prokes, V. G. de Paula, H. N. Bordallo, A. Maljuk, S. Landsgesell, H. Ryll, B. Klemke, S. Paeckel, K. Kiefer, K. Lefmann, L. T. Kuhn, and D. N. Argyriou, Nat. Mater. **11**, 694 (2012).
[7] Y. Tokunaga, S. Iguchi, T. Arima, and Y. Tokura, Phys. Rev. Lett. **101**, 097205 (2008).
[8] Y. Tokunaga, Y. Taguchi, T. Arima, and Y. Tokura, Nat. Phys. **8**, 558 (2009).
[9] J.-H. Lee, Y. K. Jeong, J. H. Park, M.-A. Oak, H. M. Jang, J. Y. Son, and J. F. Scott, Phys. Rev. Lett. **107**, 117201 (2011).
[10] A. V. Kimel, A. Kirilyuk, A. Tsvetkov, R. V. Pisarev, and Th. Rasing. Nature (London) **429**, 850 (2004).
[11] A. V. Kimel, C. D. Stanciu, P. A. Usachev, R. V. Pisarev, V. N. Gridnev, A. Kirilyuk, and Th. Rasing, Phys. Rev. B **74**, 060403(R) (2006).
[12] J. A. de Jong, A. V. Kimel, R. V. Pisarev, A. Kirilyuk, and Th. Rasing, Phys. Rev. B **84**, 104421 (2011).
[13] J. A. de Jong, I. Razdolski, A. M. Kalashnikova, R. V. Pisarev, A. M. Balbashov, A. Kirilyuk, Th. Rasing, and A. V. Kimel, Phys. Rev. Lett. **108**, 157601 (2012).
[14] A. V. Kimel, A. Kirilyuk, P. A. Usachev, R. V. Pisarev, A. M. Balbashov, and Th. Rasing, Nature (London) **435**, 655 (2005).
[15] T. Satoh, S.-J. Cho, R. Iida, T. Shimura, K. Kuroda, H. Ueda, Y. Ueda, B. A. Ivanov, F. Nori, and M. Fiebig, Phys. Rev. Lett. **105**, 077402 (2010).
[16] R. Iida, T. Satoh, T. Shimura, K. Kuroda, B. A. Ivanov, Y. Tokunaga, and Y. Tokura, Phys. Rev. B **84**, 064402 (2011).

[17] A. V. Kimel, B. A. Ivanov, R. V. Pisarev, P. A. Usachev, A. Kirilyuk, and Th. Rasing, Nat. Phys. **5**, 727 (2009).
[18] B. Koopmans, M. van Kampen, J. T. Kohlhepp, and W. J. M. de Jonge, Phys. Rev. Lett. **85**, 844 (2000).
[19] G. P. Zhang, W. Hübner, G. Lefkidis, Y. Bai, and T. F. George, Nat. Phys. **5**, 499 (2009).
[20] K. Carva, M. Battiato, and P. M. Oppeneer, Nat. Phys. **7**, 665 (2011).
[21] R. V. Mikhaylovskiy, E. Hendry, and V. V. Kruglyak, Phys. Rev. B **86**, 100405(R) (2012).
[22] K. Yamaguchi, M. Nakajima, and T. Suemoto, Phys. Rev. Lett. **105**, 237201 (2010).
[23] R. Zhou, Z. Jin, G. Li, G. Ma, Z. Cheng, and X. Wang, Appl. Phys. Lett. **100**, 061102 (2012).
[24] Z. Jin, Z. Mics, G. Ma, Z. Cheng, M. Bonn, and D. Turchinovich, Phys. Rev. B **87**, 094422 (2013).
[25] K. Yamaguchi, T. Kurihara, Y. Minami, M. Nakajima, and T. Suemoto, Phys. Rev. Lett. **110**, 137204 (2013).
[26] J. Jiang, Z. Jin, G. Song, X. Lin, G. Ma, and S. Cao, Appl. Phys. Lett. **103**, 062403 (2013).
[27] R. V. Mikhaylovskiy, E. Hendry, F. Y. Ogrin, and V. V. Kruglyak, Phys. Rev. B **87**, 094414 (2013).
[28] T. Kampfrath, A. Sell, G. Klatt, A. Pashkin, S. Mährlein, Th. Dekorsy, M. Wolf, M. Fiebig, A. Leitenstorfer, and R. Huber, Nat. Photonics **5**, 31 (2011).
[29] E. Beaurepaire, G. M. Turner, S. M. Harrel, M. C. Beard, J.-Y. Bigot, and C. A. Schmuttenmaer, Appl. Phys. Lett. **84**, 3465 (2004).
[30] D. J. Hilton, R. D. Averitt, C. A. Meserole, G. L. Fisher, D. J. Funk, J. D. Thompson, and A. J. Taylor, Opt. Lett. **29**, 1805 (2004).
[31] T. Kampfrath, M. Battiato, P. Maldonado, G. Eilers, J. Nötzold, S. Mährlein, V. Zbarsky, F. Freimuth, Y. Mokrousov, S. Blügel, M. Wolf, I. Radu, P. M. Oppeneer, and M. Münzenberg, Nat. Nanotechnol. **8**, 256 (2013).
[32] J. Nishitani, K. Kozuki, T. Nagashima, and M. Hangyo, Appl. Phys. Lett. **96**, 221906 (2010).
[33] T. Higuchi, N. Kanda, H. Tamaru, and M. Kuwata-Gonokami, Phys. Rev. Lett. **106**, 047401 (2011).
[34] N. Kanda, T. Higuchi, H. Shimizu, K. Konishi, K. Yoshioka, and M. Kuwata-Gonokami, Nat. Commun. **2**, 362 (2011).
[35] J. Nishitani, T. Nagashima, and M. Hangyo, Phys. Rev. B **85**, 174439 (2012).
[36] J. Nishitani, T. Nagashima, and M. Hangyo, Appl. Phys. Lett. **103**, 081907 (2013).
[37] J. Li, T. Higuchi, N. Kanda, K. Konishi, S. G. Tikhodeev, and M. Kuwata-Gonokami, Opt. Express **19**, 22550 (2011).
[38] K. P. Belov, A. K. Zvezdin, A. M. Kadomtseva, and R. Z. Levitin, Sov. Phys. Usp. **19**, 574 (1976).
[39] *High Frequency Processes in Magnetic Materials*, edited by G. Srinivasan and A. N. Slavin (World Scientific Publishing, Singapore, 1995).
[40] Z. Y. Zhao, X. Zhao, H. D. Zhou, F. B. Zhang, Q. J. Li, C. Fan, X. F. Sun, and X. G. Li, Phys. Rev. B **89**, 224405 (2014).
[41] To estimate the steady-state temperature buildup we use the Fourier law of heat conduction $W \approx -kS(\Delta T/\Delta l)$, where W is average power absorbed in the sample, κ is the thermal conductivity and $S = 2\pi rd$ is the area of the excited region of the sample, $r \approx 1$ mm and $d = 60$ μm being radius of the pump spot and the sample thickness respectively. $\Delta T = T_0 - T$ is the difference between the temperature of the unexcited area T_0 which is read by the thermocouple and the temperature of the excited area T;Δl is a characteristic distance between the excited region of the sample and equilibrium region. For a rough estimate we assume $\Delta l = r$. By taking $W = 100$ mW, $\kappa \approx 30$ W/K m [40] we get $\Delta T \approx 10$ K.
[42] R. V. Mikhaylovskiy, E. Hendry, A. Secchi, J. H. Mentink, M. Eckstein, A. Wu, R. V. Pisarev, V. V. Kruglyak, M. I. Katsnelson, Th. Rasing, and A. V. Kimel (unpublished).
[43] B. A. Ivanov, Low Temp. Phys. **40**, 91 (2014).
[44] G. F. Herrmann, Phys. Rev. **133**, A1334 (1964).
[45] D. L. Wood, L. M. Holmes, and J. P. Remeika, Phys. Rev. **185**, 689 (1969).
[46] A. P. Malozemoff, J. Phys. Chem. Solids **32**, 1669 (1971).
[47] A. M. Balbashov, A. A. Volkov, G. V. Kozlov, S. P. Lebedev, A. A. Mukhin, A. Yu. Pronin, A. S. Prokhorov, and A. M. Prokhorov, JETP Lett. **42**, 564 (1985).
[48] A. M. Balbashov, A. G. Berezin, Yu. V. Bobryshev, P. Yu. Marchukov, I. V. Nikolaev, Ya. Paches, L. Pust, E. G. Rudashevskii, and V. V. Shushpanov, Zh. Eksp. Teor. Fiz. **102**, 1397 (1992) [Sov. Phys. JETP **75**, 757 (1992)].
[49] A. A. Mukhin, A. N. Lobanov, M. Goiran, J. Leotin, and A. A. Volkov, J. Magn. Reson. **195**, 60 (2008).